

NASA Contractor Report CR-201354

**Verification and Implementation of Microburst Day Potential Index (MDPI) and Wind INDEX (WINDEX) Forecasting Tools at Cape Canaveral Air Station**

Prepared By:  
*Applied Meteorology Unit*

Prepared for:  
Kennedy Space Center  
Under Contract NAS10-11844

NASA  
National Aeronautics and  
Space Administration

Office of Management

Scientific and Technical  
Information Program

1996



**ATTRIBUTES AND ACKNOWLEDGMENTS:**

Dr. Francis J. Merceret  
PH-B3

**Applied Meteorology Unit (AMU):**

Mark Wheeler, Author

---

## TABLE OF CONTENTS

ATTRIBUTES AND ACKNOWLEDGMENTS: .....	i
TABLE OF CONTENTS.....	ii
LIST OF TABLES .....	iii
LIST OF FIGURES .....	iv
1. INTRODUCTION.....	1
2. CASE STUDY AND BACKGROUND.....	1
2.1 Synoptic Weather Analysis.....	5
2.2 KSC/CCAS Wind Tower Data Analysis.....	5
2.3 WSR-88D Radar Analysis .....	8
3. MDPI AND WINDEX IMPLEMENTATION .....	13
3.1 MDPI.....	13
3.2 WINDEX.....	13
3.3 Development of Utilities .....	14
3.4 Detection: Nowcasting Techniques .....	16
4. VERIFICATION TECHNIQUES AND RESULTS.....	16
4.1 MDPI Verification .....	16
4.2 Nowcasting Signatures Verification.....	17
4.3 WINDEX Verification.....	25
5. RECOMMENDATIONS.....	26
6. SUMMARY.....	26
7. REFERENCES .....	26

**LIST OF TABLES**

Table 1. Predicted Condition vs. Observed Microburst .....	17
Table 2. Computed WINDEX Microburst Gust vs. Observed Gust.....	25

## LIST OF FIGURES

Figure 1. KSC and CCAS map with points of interest. ....	2
Figure 2. Thermodynamic profile of $\theta_e$ for 16 August (microburst) and 10 August 1994 (typical summer non-microburst $\theta_e$ profile). ....	3
Figure 3. WSR-88D vertical cross section of thunderstorm at 2031 UTC on 16 August 1994 (precipitation core is highlighted). ....	4
Figure 4. WSR-88D base reflectivity PPI at 0.4° elevation at 2031 UTC on 16 August 1994 (Cell that produced a wet microburst is highlighted). ....	6
Figure 5. SLF wind sensor 1-minute peak wind speed between 2012 and 2100 UTC on 16 August 1994. ....	7
Figure 6. SLF wind tower plot at 2048 indicating a starburst wind pattern associated with the wet microburst. ....	8
Figure 7. Demonstration of how convection is initiated when HCRs (small rolls) interact with the SBF (larger roll) (from Atkins et. al. 1995). ....	9
Figure 8. Developing HCRs (white arrows) associated with the southwest surface flow, WSR-88D base reflectivity PPI at 0.4° elevation at 1631 UTC on 16 August 1994. ....	10
Figure 9. Enhanced HCRs (white arrows) displayed on WSR-88D base reflectivity PPI at 0.4° elevation at 1943 UTC on 16 August 1994. ....	11
Figure 10. WSR-88D reflectivity cross-section of the cell to the southwest of the SLF at 2041 UTC on 16 August 1994 (precipitation core is highlighted). ....	13
Figure 11. Example of MIDDs graphical MDPI/WINDEX display. ....	<b>Error! Bookmark not defined.</b>
Figure 12. WSR-88D VIL at 2036 UTC on 26 June 1995. ....	19
Figure 13. WSR-88D reflectivity cross-section at 2036 UTC on 26 June 1995 (precipitation core is highlighted). ....	20
Figure 14. WSR-88D VIL at 2223 UTC on 10 July 1995 (46 dBZ VIL core center is highlighted). ....	21
Figure 15. WSR-88D reflectivity cross-section at 2223 UTC 10 July 1995 (precipitation core highlighted). ....	22
Figure 16. WSR-88D VIL at 1949 UTC on 8 September 1995 (46 dBZ VIL core center is highlighted). ....	23
Figure 17. WSR-88D reflectivity cross-section at 1949 UTC on 8 September 1995 (precipitation core is highlighted). ....	24

## 1. INTRODUCTION

The purpose of this report is to document the development and verification of the Applied Meteorology Unit's (AMU) and 45th Weather Squadron's (45 WS) Microburst Day Potential Index (MDPI) and Wind INDEX (WINDEX) forecasting tools. MDPI and WINDEX are defined in Section 3. The AMU was tasked to:

- Develop a Meteorological Interactive Data Display System (MIDDS) MDPI and WINDEX utility that would heighten the awareness of the duty forecaster to the potential of wet microbursts and gust maxima,
- Validate the MDPI technique and WINDEX gust potential values with data from June through September 1995, and
- Transition techniques to operational use.

The following sections describe the AMU's development, implementation, and verification of the MDPI and WINDEX forecaster tools. Section 2 describes the case study and supporting background which lead to the development of the MDPI, and Section 3 describes the implementation of the MDPI during the summer of 1995. Section 4 discusses the verification techniques and results and Section 5 contains AMU recommendations. Sections 6 and 7 contain the summary and list of references, respectively.

## 2. CASE STUDY AND BACKGROUND

On 16 August 1994, the Kennedy Space Center (KSC) and Cape Canaveral Air Station (CCAS) area experienced several strong downrush wind events. The events started at 2000 UTC near the NASA causeway and continued east-northeastward across KSC through 2100 UTC. The strongest unforecast wind gusts of  $33.5 \text{ ms}^{-1}$  (65 kt) were reported at the Shuttle Landing Facility (SLF) between 2030 and 2050 UTC (Figure 1).

After this event, the 45 WS suspected that a wet microburst was responsible for the unexpectedly high winds (Roeder 1994a). The 45 WS requested that the AMU perform a detailed analysis of the environmental conditions leading up to the events on 16 August 1994. The AMU later confirmed through a technical analysis of the mesoscale wind tower network, rawinsonde, radar, and satellite data that a wet microburst had caused the severe winds. A microburst is defined as a small scale, low altitude, intense downdraft which impacts the surface and cause strong divergent outflows of wind (Wolfson 1990).

Previous studies of dry microbursts have resulted in a conceptual model depicting the thermodynamic structure of a dry microburst for the High Plains (Wakimoto 1985). Wakimoto and Bringi (1988) showed that a different class of microbursts (i.e. wet microbursts) exist for areas that experience moderate to heavy convective rains. During the 1986 MIST (Microburst and Severe Thunderstorm) project conducted in northern Alabama, Atkins and Wakimoto (1991) collected data from several wet microbursts and documented the general environmental conditions that favor these events.

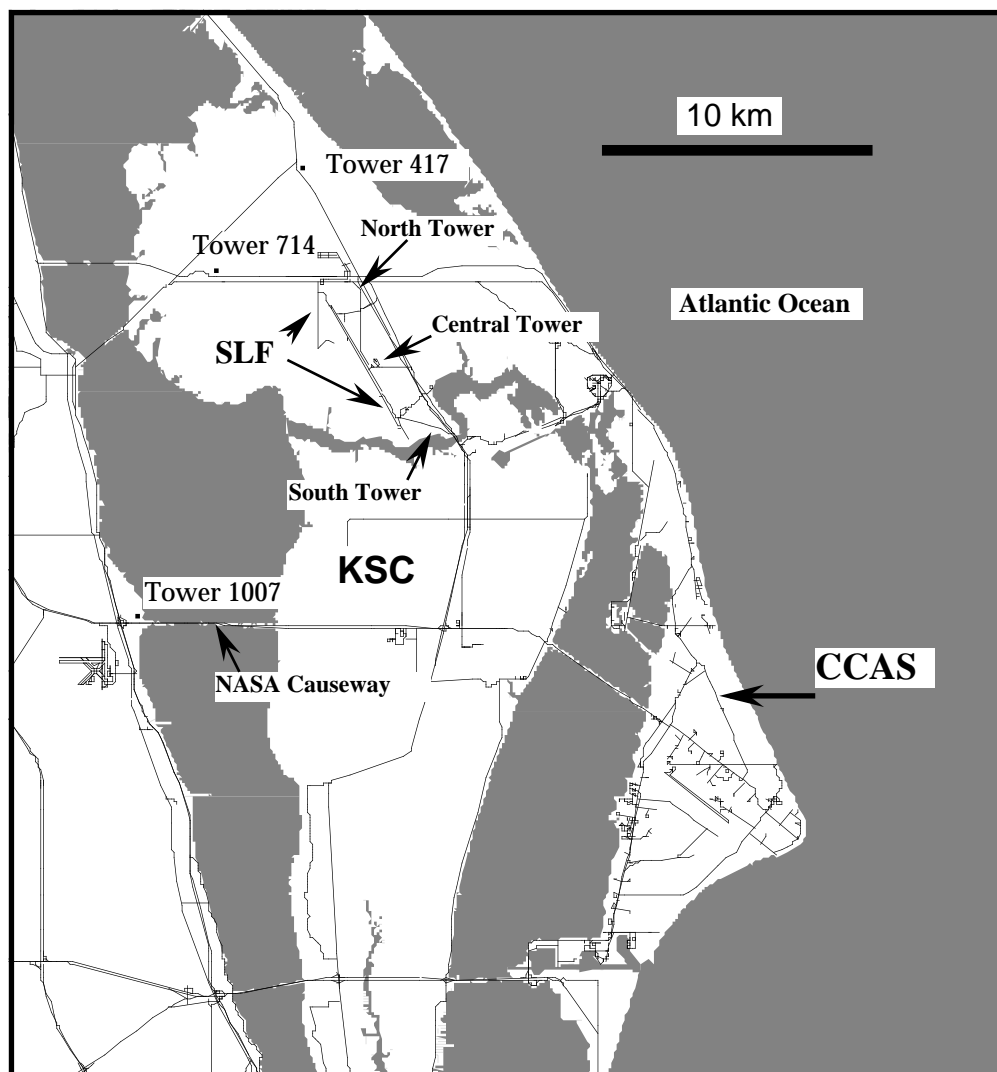


Figure 1. KSC and CCAS map with points of interest.

Atkins and Wakimoto's analysis of the thermodynamic structure of the wet microburst days indicated that it was possible to differentiate between normal thunderstorm days and potential wet microburst days by plotting the vertical profile of the equivalent potential temperature,  $\theta_e$  (Figure 2). By analyzing the difference between the surface  $\theta_e$  and the minimum  $\theta_e$  value at some height aloft, it is possible to determine if there is a reasonable potential for wet microburst thunderstorms. From the research during the MIST project, Atkins and Wakimoto proposed that if the difference of the surface  $\theta_e$  value and the minimum  $\theta_e$  value aloft is greater than or equal to  $20^\circ\text{K}$  (Kelvin) then there is a high potential for wet microbursts given that thunderstorms are forecast. If the difference of the surface value of the  $\theta_e$  and the minimum  $\theta_e$  value aloft is less than  $13^\circ\text{K}$ , wet microbursts are much less likely.

At least two of the local storms on 16 August 1994 met the criteria experts have established as wet microburst signatures. The  $\theta_e$  profile from the late morning Cape Canaveral rawinsonde was characterized by a large decrease in the  $\theta_e$  in the lowest 4.3 km (14000 ft) of the atmosphere. This type of environment is considered conducive for the development of wet microbursts.

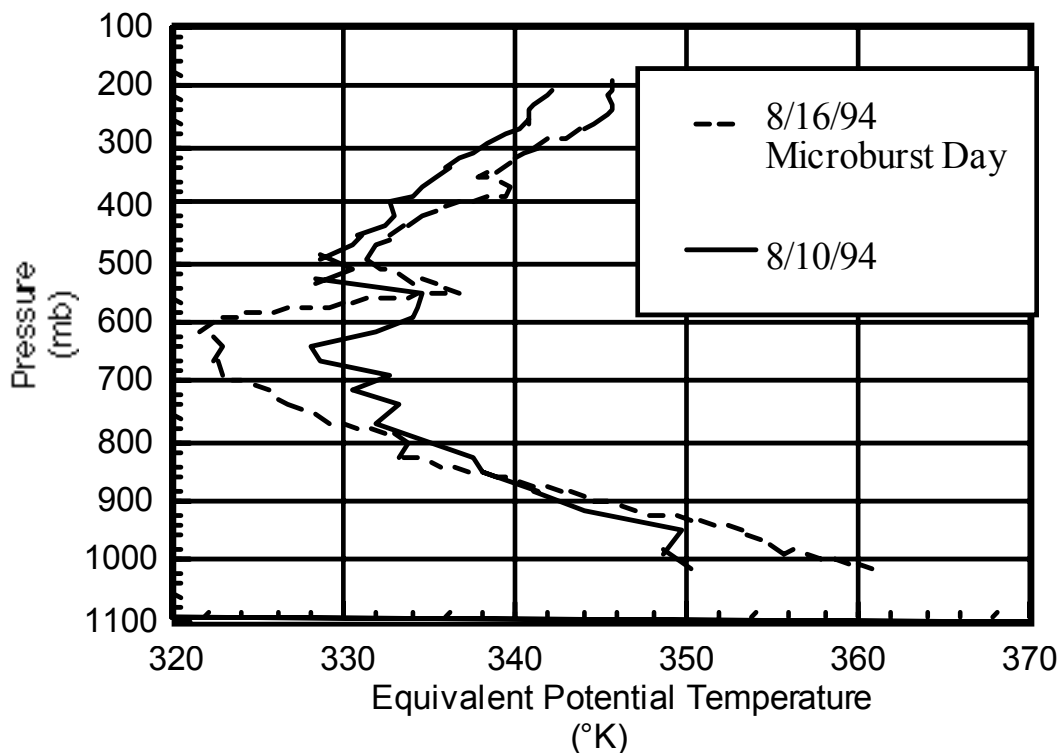


Figure 2. Thermodynamic profile of  $\theta_e$  for 16 August (microburst) and 10 August 1994 (typical summer non-microburst  $\theta_e$  profile).

During the analysis of Doppler radar data from the microburst events in the MIST project, Atkins and Wakimoto (1991) noted an important nowcasting signature in the vertical storm structure. They observed that the height of the main precipitation maximum reflectivity (core) relative to the height of the minimum  $\theta_e$  within the main storm structure is important to the development of wet microbursts. In all radar-observed wet microburst events, this core consistently reached the levels of minimum  $\theta_e$  and the upper portion of this core reached heights of 7 km (23000 ft) (dry region above 500 mb). This upper core consists mostly of ice.

Analysis of the WSR-88D 2031 UTC vertical radar reflectivity values on 16 August 1994 show that the main precipitation core reached an altitude of 5.4 km (17500 ft), which was into the layer of dry air aloft (Figure 3). The lapse of  $\theta_e$  and structure of the precipitation core both indicate that the local storms on 16 August 1994 met Atkins and Wakimoto criteria for their classification of wet microburst events.

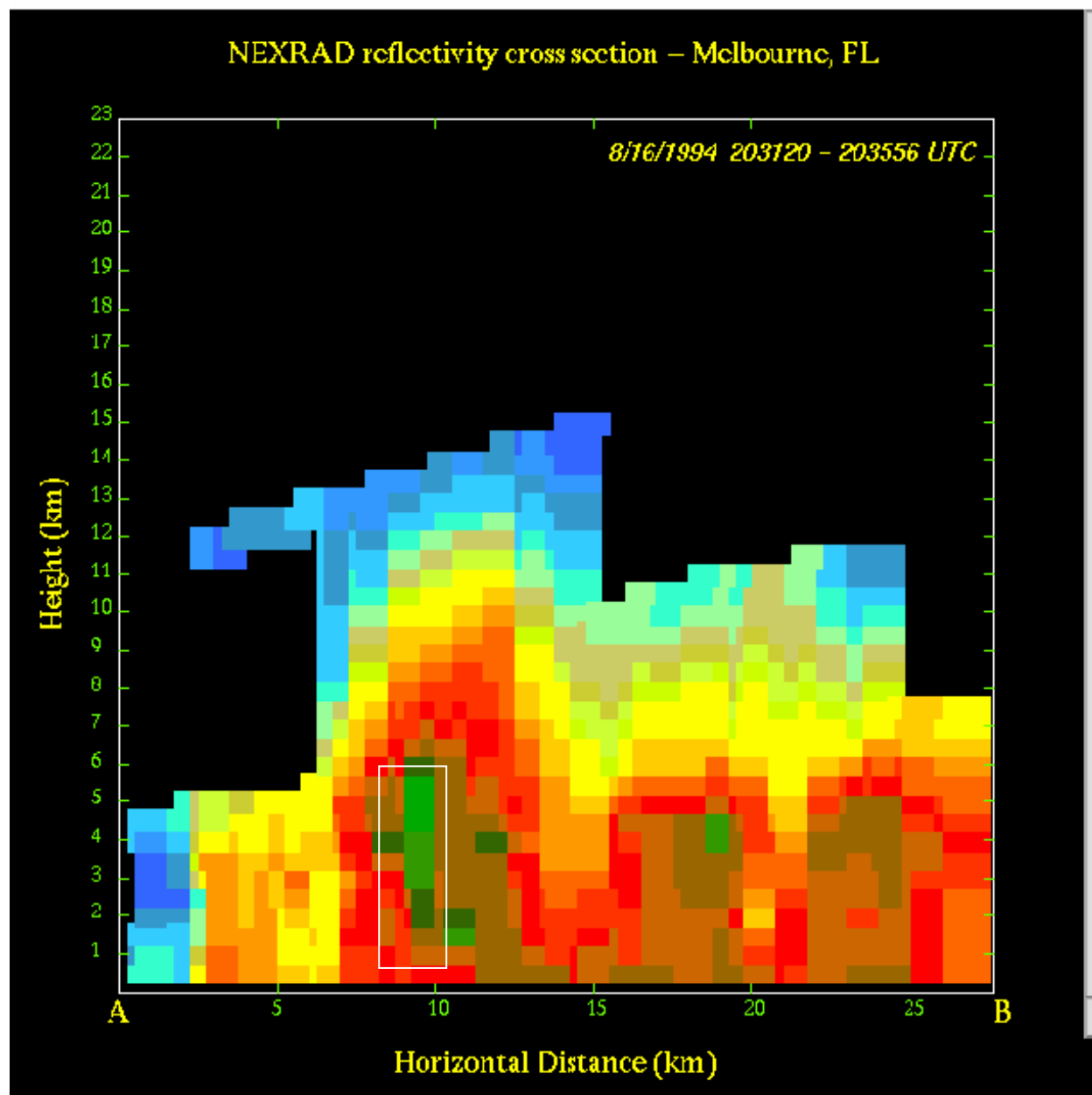


Figure 3. WSR-88D vertical cross section of thunderstorm at 2031 UTC on 16 August 1994 (precipitation core is highlighted).

## 2.1 *Synoptic Weather Analysis*

On the morning of 16 August 1994, the remains of Tropical Storm (TS) Beryl were centered along the southern Alabama - Georgia border. There was a 500 mb low pressure area centered over Dothan, Alabama with a strong vorticity lobe maximum from the 500 mb low pressure to west of Tampa, Florida. Satellite imagery beginning at 1200 UTC indicated several convergent lines feeding into TS Beryl, with one of the stronger feeder bands being just to the west of Tampa, Florida.

The early morning (1100 UTC) Cape Canaveral rawinsonde indicated a somewhat drier than normal atmosphere over the region with a K-Index (KI) of 22. The winds veered from the surface to 5.5 km (18000 ft) and then backed above 5.5 km (18000 ft). There was a low level speed maximum of 10.1  $\text{ms}^{-1}$  (20 kt) at 0.6 km (2000 ft). No morning rawinsonde was available from Tampa, Florida which was closer to the feeder band. The 1500 UTC Cape Canaveral rawinsonde had a low level speed maximum of 12.4  $\text{ms}^{-1}$  (24 kt) from 0.5 to 0.8 km (1500 to 2500 ft). The rawinsonde indicated that moisture had increased from the surface to 1 km (6000 ft) with another area of increased moisture between 4.3 and 5.2 km (14000 to 17000 ft). The rawinsonde showed dry air from 5.2 to 8.5 km (17000 to 28000 ft). The winds were primarily southerly from the surface to 7.6 km (25000 ft) with weak directional veering with height.

## 2.2 *KSC/CCAS Wind Tower Data Analysis*

Wind speed and direction and wind speed gusts reported every 5 minutes from 1950 to 2100 UTC were plotted over a KSC/CCAS map from the MIDD database. Also, several time-series graphs of wind speed for particular towers were analyzed. The time-series graphs were generated using the Weather Information Network Display System (WINDS) 5-minute average data and the 1-minute average data from the individual SLF wind sensors.

There were several downburst events during the period of 2000 to 2100 UTC. The first potential wet microburst event occurred at 2000 UTC near tower 1007 (see Figure 1). At the time, tower 1007 reported a gust of 16  $\text{ms}^{-1}$  (31 kt). The associated line of thunderstorms associated with the event was moving to the northeast at 7.7 to 10.3  $\text{ms}^{-1}$  (15 to 20 kt), while the thunderstorm area was moving to the east at 5  $\text{ms}^{-1}$  (10 kt). The line of cells that produced the gust at tower 1007 moved to the northeast and produced subsequent gusts of 16.5  $\text{ms}^{-1}$  (32 kt) at tower 714 and gusts of 19.0  $\text{ms}^{-1}$  (37 kt) at tower 417.

As this first line of cells moved to the east, a new cell began forming around 2013 UTC over Merritt Island. By 2030 UTC (Figure 4), this cell was near the SLF center and north wind sensors (towers 512 and 513).

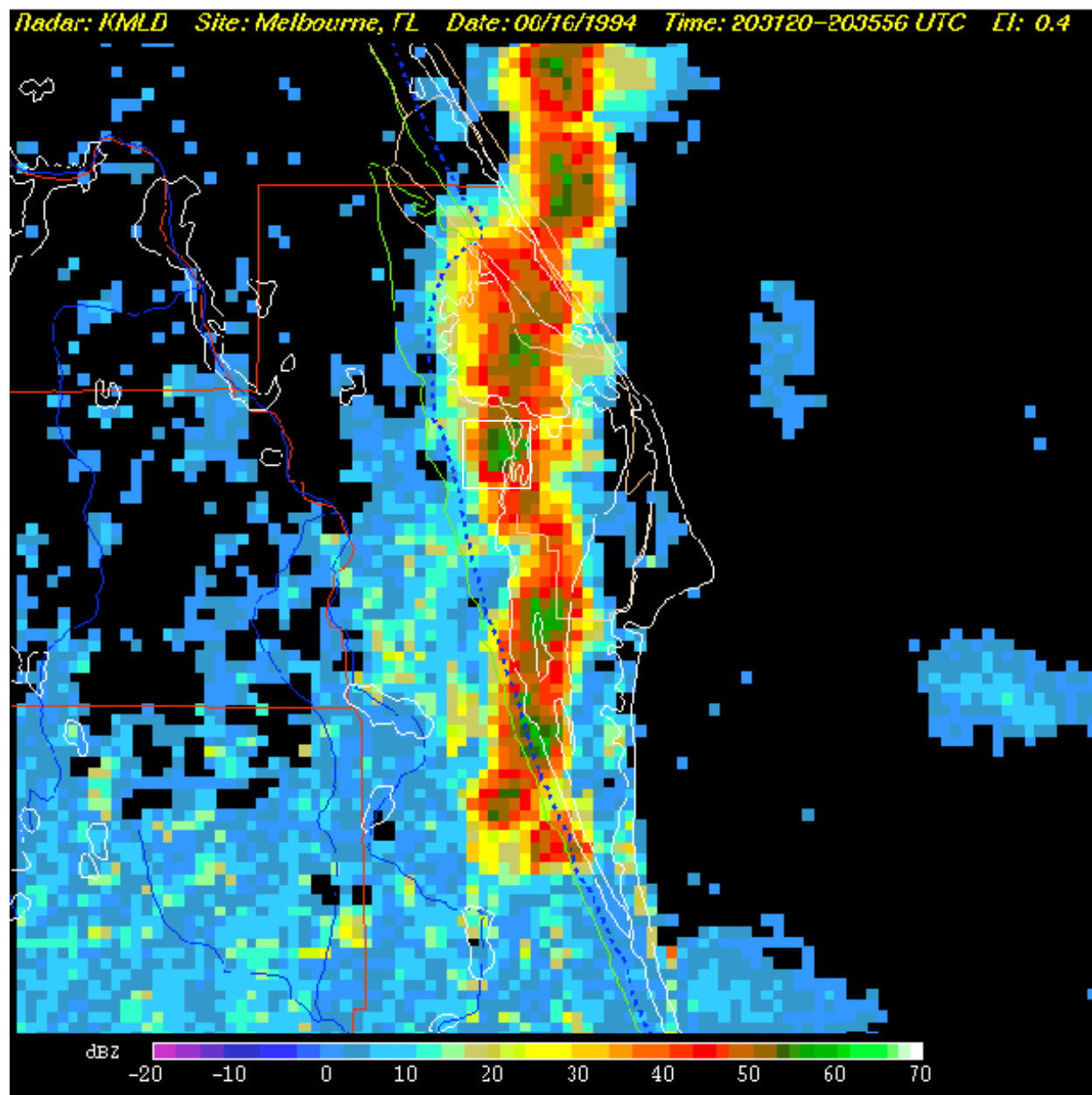


Figure 4. WSR-88D base reflectivity PPI at 0.4° elevation at 2031 UTC on 16 August 1994 (Cell that produced a wet microburst is highlighted).

At 2030 UTC, tower 513 reported a 35° wind shift (from 220° to 185°) to a more southerly flow with a wind gust of 26.8 ms<sup>-1</sup> (52 kt) (Figure 5). At this same time, tower 512 reported a small 16° wind shift (from 278° to 262°) and remained westerly with a gust of 19.6 ms<sup>-1</sup> (38 kt). This downburst wind divergent outflow pattern was consistent with Fujita's microburst criteria of damaging winds extending only 4 km (2.5 miles) or less (Fujita 1985).

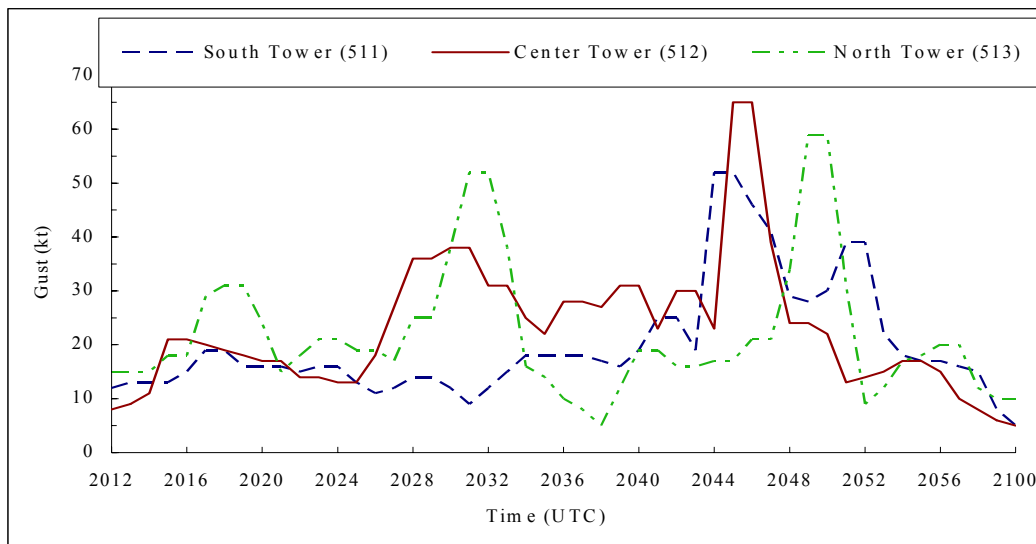


Figure 5. SLF wind sensor 1-minute peak wind speed between 2012 and 2100 UTC on 16 August 1994.

Also at 2031 UTC, a new cell (Figure 4) began developing on the southern portion of the cell which produced the microburst. By 2045 UTC this new cell moved northeast toward the SLF. Between 2044 and 2050 UTC all three wind sensors at the SLF reported winds greater than 25.7 ms<sup>-1</sup> (50 kt) (Figure 5). The wind barb plot is characterized by a starburst pattern indicating that a wet microburst event occurred just west of the south and center sensors with most of the energy moving with the environmental wind and cell motion to the northeast.

As in the previous wet microburst event, the divergent and spatial resolution satisfied Fujita's diameter and horizontal length microburst criteria. Analysis of the 1-minute average wind data from 2047 to 2050 UTC from each wind sensor indicates the following:

- The north SLF wind sensor reported a shift to a more south-southwest flow (156° to 195°) with a gust of 30.4 ms<sup>-1</sup> (59 kt),
- The center SLF wind sensor reported a wind shift of 14° (from 184° to 198°) and a gust of 33.5 ms<sup>-1</sup> (65 kt), and
- The south SLF wind sensor reported a more northwesterly shift in wind direction (246° to 279°) and a gust of 26.8 ms<sup>-1</sup> (52 kt) indicating a starburst (divergent) wind pattern.

The wind barb plots for the north, central, and south SLF wind sensors during the time of the microbursts (2030 and 2048 UTC) indicated a starburst divergent pattern (Figure 6) with a diameter less than 4 km (2.5 miles). Graphs of SLF wind tower time versus wind speed as a function of time profiles (Figure 5) were also similar to those Fujita found typical of microburst events (i.e. a mound-shaped appearance lasting 2 to 5 minutes) (Fujita 1985).

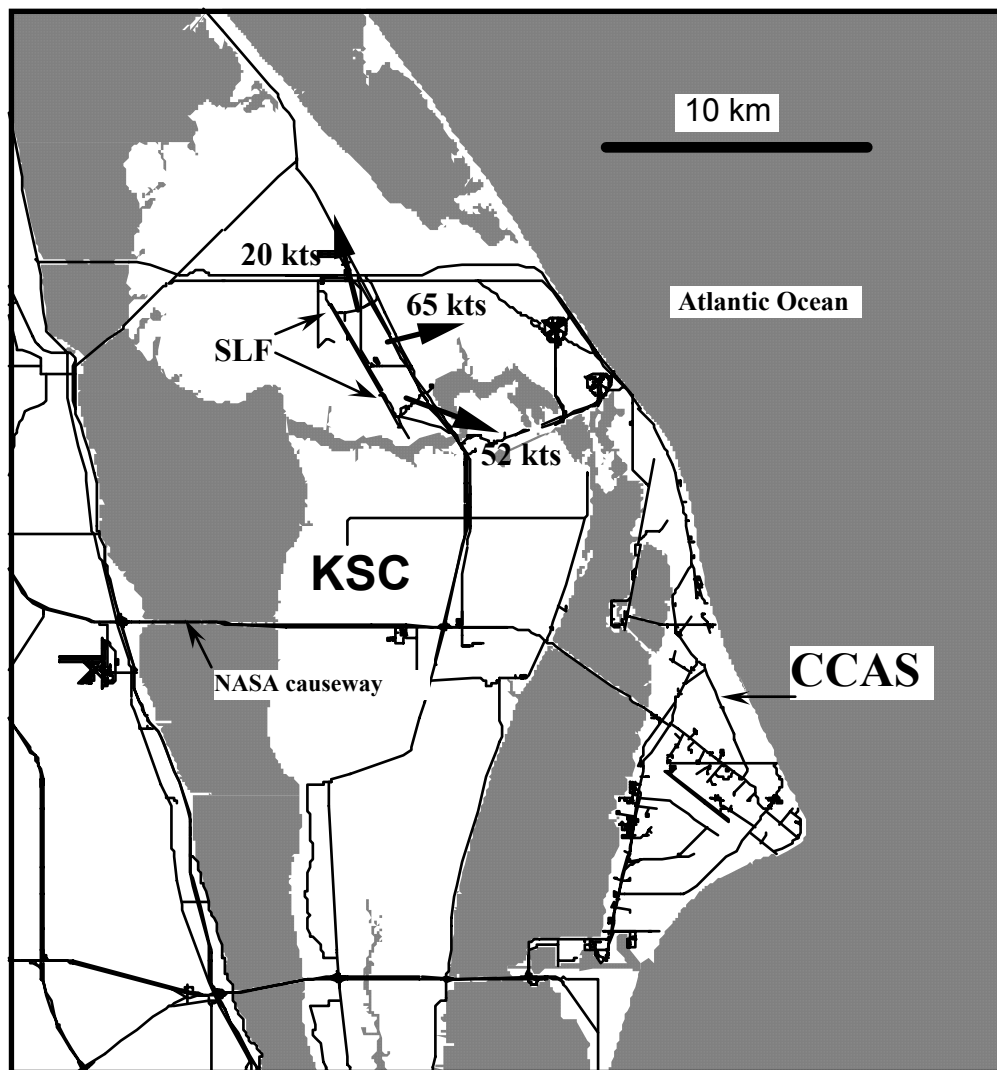


Figure 6. SLF wind tower plot at 2048 indicating a starburst wind pattern associated with the wet microburst.

### 2.3 WSR-88D Radar Analysis

For this study, WSR-88D level II base data products were available for analysis from 1330 to 2300 UTC on 16 August 1994. These products were provided by the National Weather Service Melbourne, Florida office (NWS MLB). IRAS, a NEXRAD base data display program, was used to display and analysis the radar data.

The purpose of the AMU's analysis of the NWS MLB's WSR-88D data was to understand the relationship between the storm structure, the environmental thermodynamic structure, and the identification of the wet microburst events in the wind tower data.

The initial convection on 16 August 1994 started by the interaction between horizontal convective rolls (HCRs) and the sea breeze front (SBF). HCRs are a common form of boundary layer convection consisting of counterrotating helices aligned nearly parallel to the mean boundary layer wind flow (Atkins and Wakimoto 1995). With the increased convergence and vertical motion caused by the

---

interaction of the HCRs and the SBF (Figure 7), increased thunderstorm development began just southwest of the Cape Canaveral area.

Figure 7. Demonstration of how convection is initiated when HCRs (small rolls) interact with the SBF (larger roll) (from Atkins et. al. 1995).

Analysis of the WSR-88D reflectivity products from 1631 and 1943 UTC (Figures 8 and 9) indicate that the initial convection developed from the interaction of the SBF and HCRs. By 1943 UTC, cells were developing along the convergent line extending from west of Melbourne to the KSC Headquarters area and then northward into the Atlantic Ocean.

Analysis of the 2041 UTC WSR-88D reflectivity patterns indicates the precipitation core (Figure 10) for the first SLF wet microburst event which occurred at 2041 UTC extended up to the mid-level dry air at 5.5 km (18000 ft). At 5.4 km (17700 ft) over KSC, the maximum reflectivity was approximately 55 dBZ. However, at 6 km (19600 ft) the reflectivity maximum drops to about 30 to 35 dBZ as can be seen in the vertical cross section (Figure 10) (See Section 3.4 for WSR-88D nowcasting signatures).

Analyses of the 2048 UTC WSR-88D reflectivity patterns at 4.3° and 6.0° elevation scans showed a similar nowcasting signature. The radar data analysis indicated a reflectivity maximum of 50 to 55 dBZ at 5.2 km (17000 ft) while at 6 km (19600 ft) on the vertical cross section showed a weaker maximum of 32 to 38 dBZ.

Thus, in both cases the main precipitation core had a similar structure to what Atkins and Wakimoto had observed in wet microburst events in the MIST project.

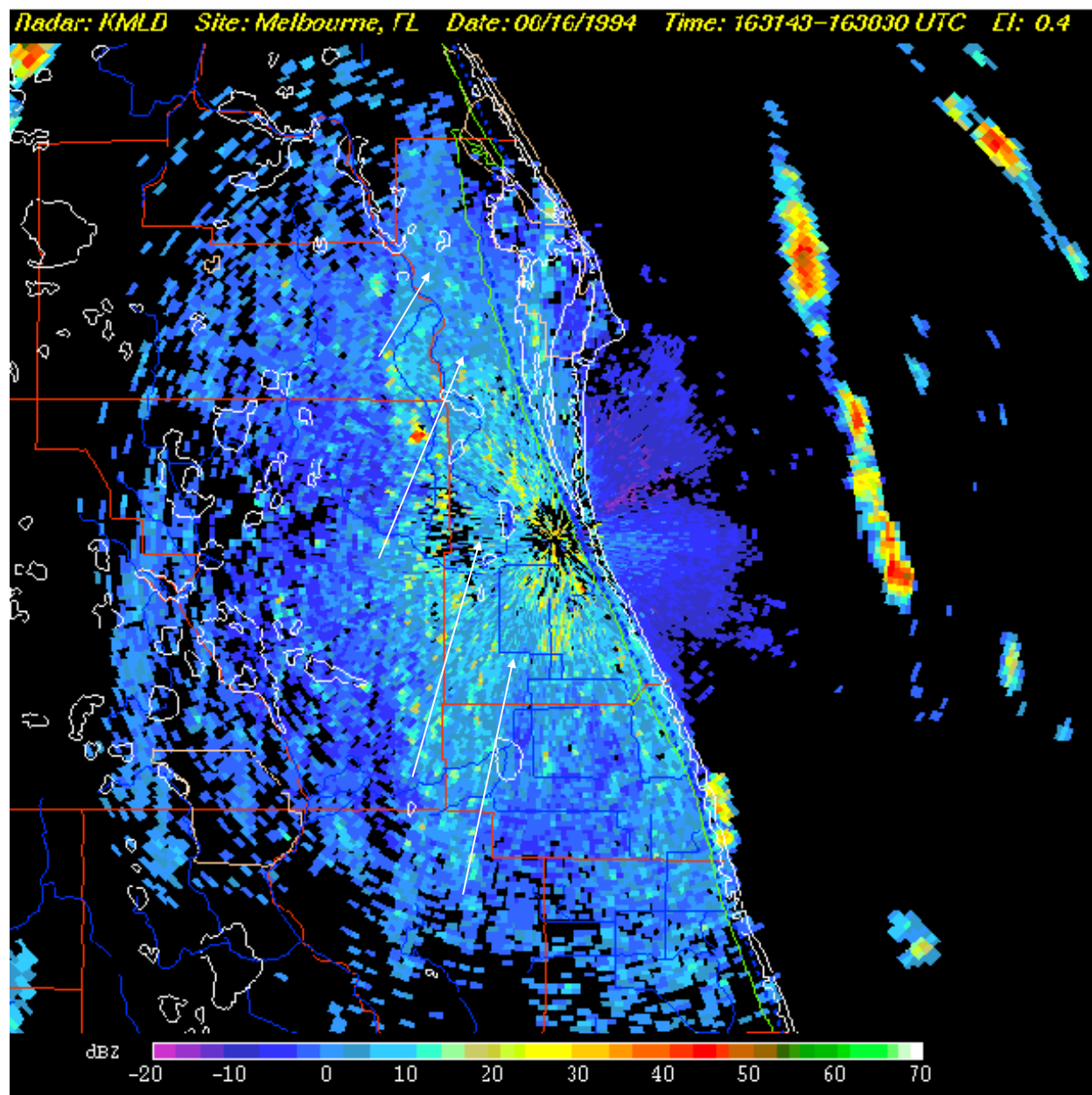


Figure 8. Developing HCRs (white arrows) associated with the southwest surface flow, WSR-88D base reflectivity PPI at 0.4° elevation at 1631 UTC on 16 August 1994.

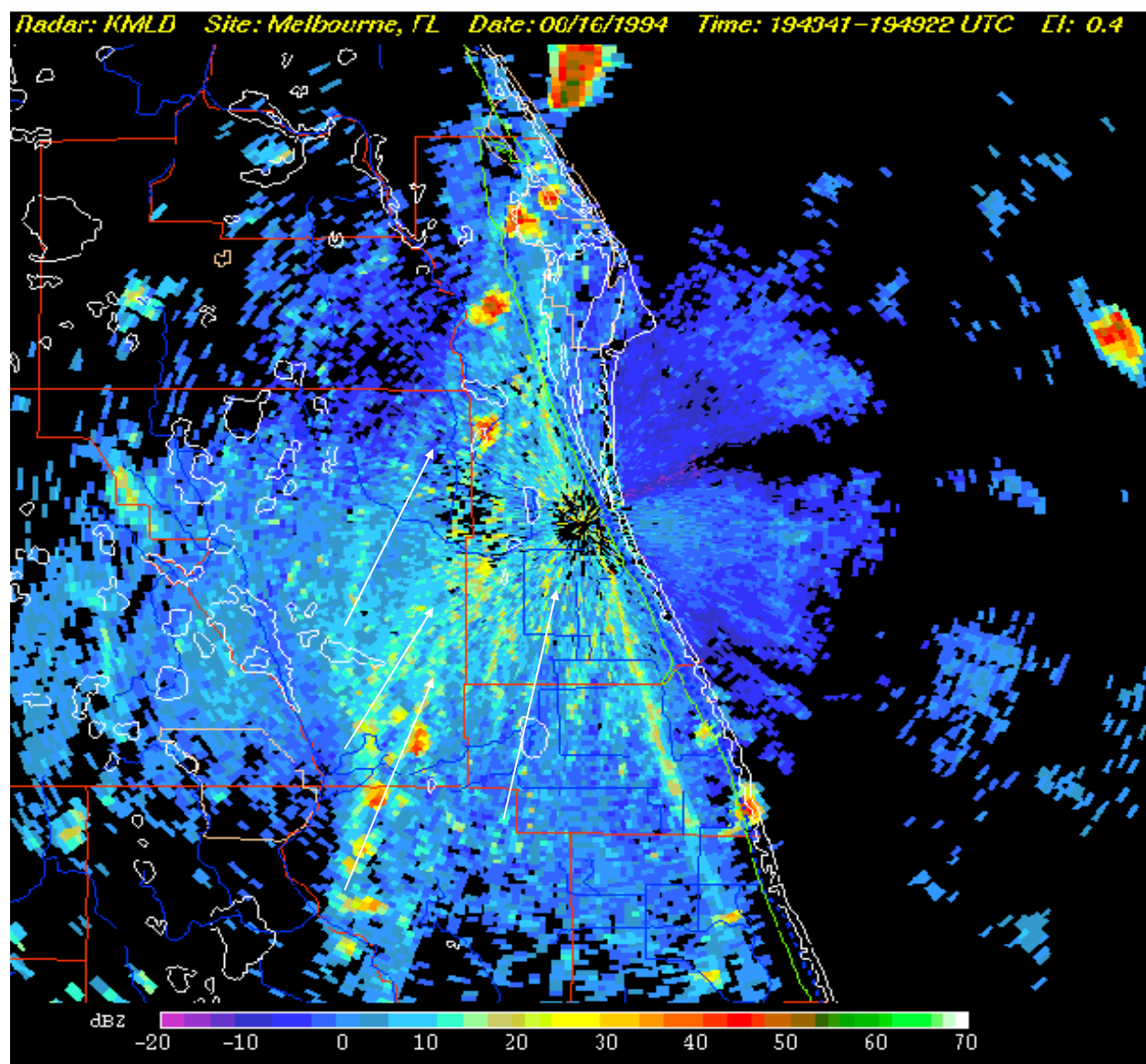


Figure 9. Enhanced HCRs (white arrows) displayed on WSR-88D base reflectivity PPI at 0.4° elevation at 1943 UTC on 16 August 1994.

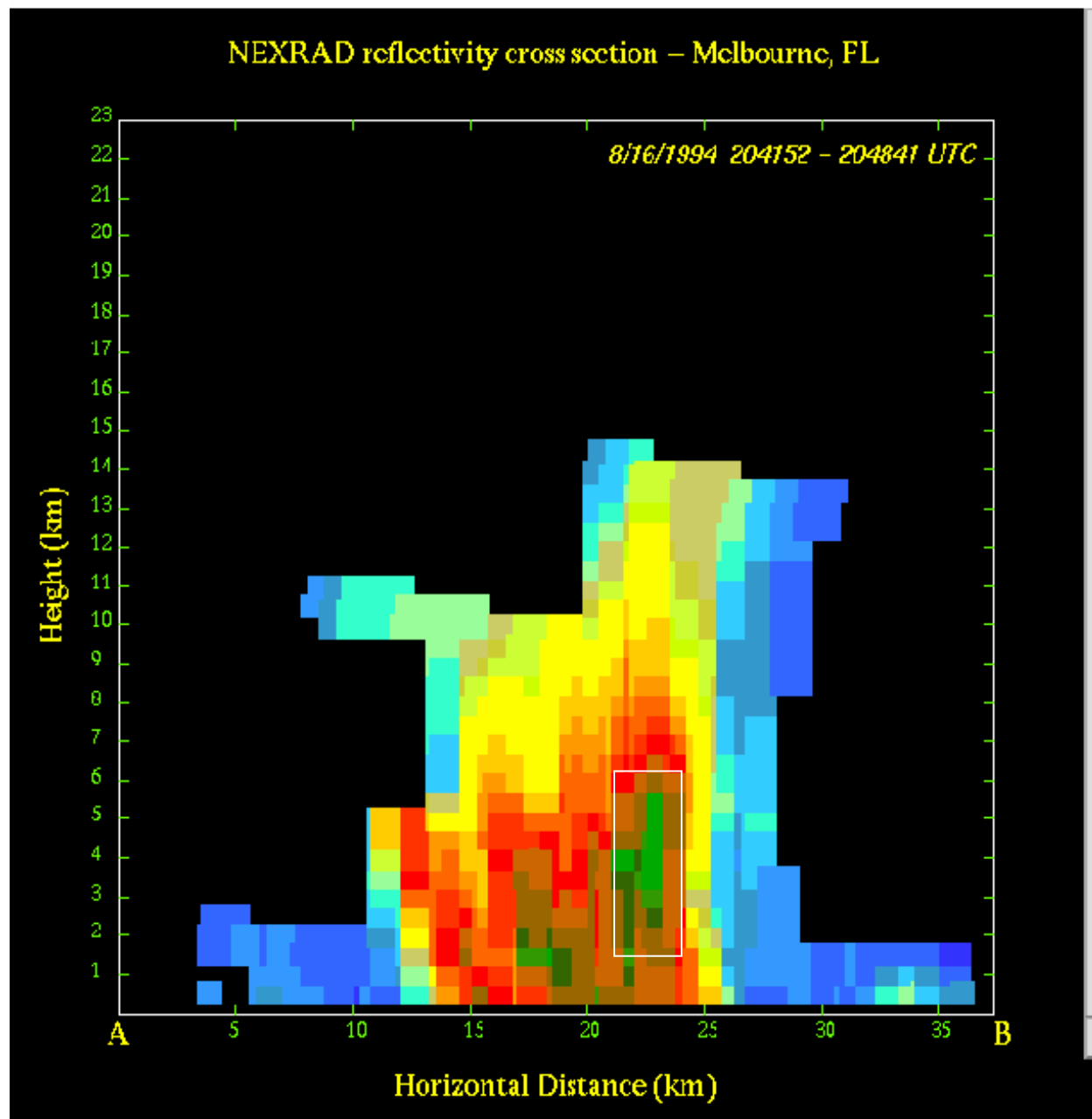


Figure 10. WSR-88D reflectivity cross-section of the cell to the southwest of the SLF at 2041 UTC on 16 August 1994 (precipitation core is highlighted).

In summary, the wind mesonet data for each microburst event depicted a starburst type signature with diameters not exceeding 4 km. Examination of the wind speed time series indicated a short lived (2 to 5 minutes) gust maxima. Both of these satisfy Fujita's criteria for aerial extent, outflow pattern, and duration associated with a microburst. The  $\theta_e$  profile for 16 August 1994 displayed what Atkins and Wakimoto had determined was a classic  $\theta_e$  profile signature for wet microburst potential and the WSR-88D data showed a strong precipitation core up into the level of dry air. Since all signatures indicated that the surface wind gust produced by the thunderstorms moving over the SLF on 16 August 1994 were associated with wet microbursts, this case study was used for the development and implementation of a wet microburst forecaster aid called MDPI.

### 3. MDPI AND WINDEX IMPLEMENTATION

MDPI was proposed by the 45 WS as a wet microburst numerical probability forecast aid (Roeder 1994b). It was designed to use the  $\theta_e$  profile so that values of 1.0 or greater would suggest a high likelihood of a wet microburst event, assuming development of deep convection with moderate to heavy precipitation.

#### 3.1 MDPI

The MDPI is based on the Cape Canaveral rawinsonde  $\theta_e$  profile with

$$\text{MDPI} = (\text{Maximum } \theta_e - \text{Minimum } \theta_e \text{ aloft}) / \text{CT}.$$

- Maximum  $\theta_e$  = Maximum  $\theta_e$  in the lowest 150 mb of the rawinsonde.
- Minimum  $\theta_e$  aloft = Minimum  $\theta_e$  between 650 and 500 mb.
- CT = Critical Threshold (change in  $\theta_e$  of 30° K, locally tuned).

During the summer weather regime, early and late morning rawinsondes are necessary to determine changes in the atmosphere that could affect forecasts of thunderstorms and their potential severity. Using  $\theta_e$  profiles, a forecaster can differentiate between Central Florida environments conducive for wet microburst and non-microburst days.

The MDPI is based on the observed vertical  $\theta_e$  range (near surface  $\theta_e$  - the observed minimum  $\theta_e$  aloft) divided by the CT value of 30° K, modified locally from the results of MIST. Because of the larger surface temperature lapse on early morning CCAS rawinsondes and a more tropical air mass (Florida versus Northern Alabama), the maximum  $\theta_e$  was calculated using the lower 150 mb (Roeder 1995). After three wet microburst events, a higher CT was needed due to the airmass differences (Wheeler 1995). If thunderstorms are forecast for the day (60% or greater) and the MDPI is 1 or greater there is a high probability (> 90%) that thunderstorms moving into or forming over the KSC/CCAS may produce wet microbursts.

#### 3.2 WINDEX

WINDEX is based on studies of observed and modeled microbursts and is designed to help forecast the microburst wind gust potential (McCann 1994). WINDEX takes into account rawinsonde features such as subcloud lapse rates and low level moisture. WINDEX is more sensitive to the low-level temperature lapse rate and it is a measure of downdraft instability making WINDEX a better local

microburst potential index than other stability indices such as the Lifted Index (LI) or K-Index (KI). WINDEX values can be updated hourly by modifying the low-level rawinsonde information using hourly surface-based parameters. This modified WINDEX is more representative of the evolving boundary layer and has a definite advantage over relying on the WINDEX values calculated from the conventional rawinsondes.

### 3.3 *Development of Utilities*

The AMU developed a McBASI (McIDAS BASIC language interpreter) program that automatically computes  $\theta_e$  for each reporting level when a new Cape Canaveral rawinsonde is ingested into Meteorological Interactive Data Display System (MIDDS). The program then displays the  $\theta_e$  profile along with the current and the last previously computed MDPI value. Subsequently, in January 1996 an additional MIDDS plotting routine program called SKEWTN was received from the Space Meteorology Group at Johnson Space Flight Center in Houston, TX and was installed onto the Range Weather Operations (RWO) MIDDS. The SKEWTN program calculates and then displays the WINDEX value (in knots) based on the most current rawinsonde data. These two programs were merged into one plotting routine that calculates and displays to the forecaster a graph of the  $\theta_e$  profile. Displayed on the top of the graph is the current and previous MDPI (Figure 11).

The SKEWTN program can also be executed manually to update and display the potential gust values with each new hourly surface data observation. When the graphical display is updated, two WINDEX values are displayed. The first WINDEX value is based solely on the rawinsonde information and is displayed on the bottom line of the graphical display with the other analysis (LI, KI, etc.) values. The second WINDEX value is based on the surface observations of the closest reporting station and is displayed just above the y axis with the surface station identification and observation time (Figure 11). This allows the forecaster to monitor how changes in the surface parameters affect the WINDEX gust potential value. The forecaster now has one chart that can be monitored for the potential of wet microburst events and the associated wind gust maxima.

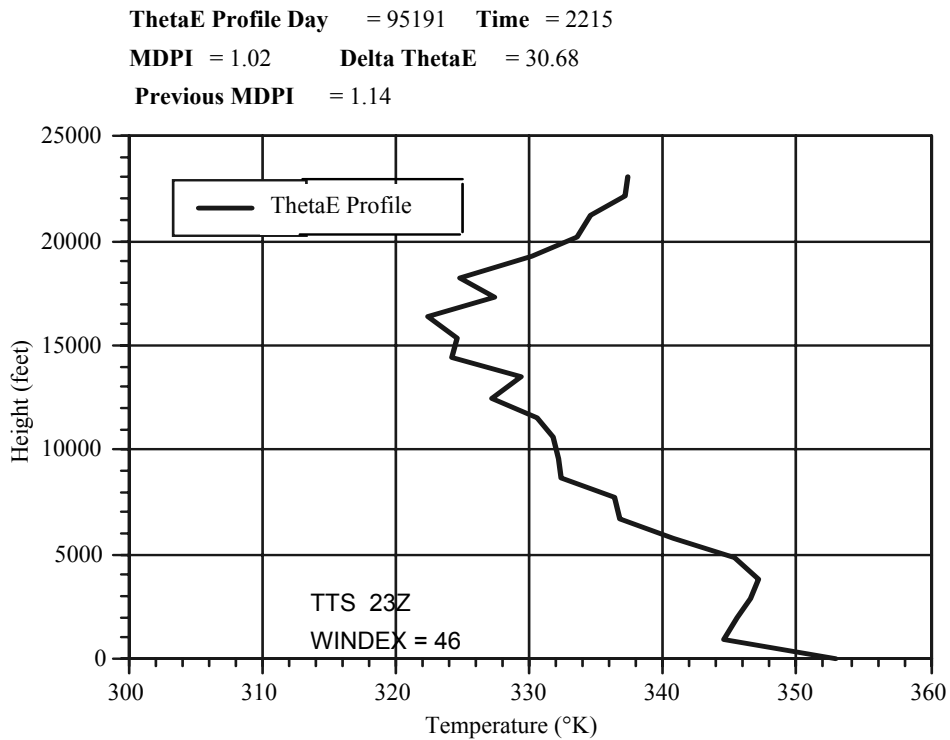


Figure 11. Example of MIDDs graphical MDPI/WINDEX display.

Figure 11 Example of MIDDs graphical MDPI/WINDEX display.

### 3.4 Detection: Nowcasting Techniques

After being informed of a potential microburst threat, the forecaster must identify which cell(s) may be of threat. The WSR-88D radar provides valuable information (precursors) that can be used to monitor what storm(s) may be of concern.

Nowcasting (< 30 minutes) techniques (Atkins and Wakimoto 1991; Eilts and Oakland 1989; Isaminger 1988) need to be used in conjunction with WSR-88D radar when thunderstorms are approaching the KSC/CCAS area. The forecaster should monitor thunderstorms for the following:

- High dBZ and/or VIL (Vertically Integrated Liquid) indicating heavy precipitation,
- A precipitation core of 55 dBZ reaching the MDPI's level of minimum  $\theta_e$ ,
- A descending precipitation core and/or divergent storm top,
- Convergence at the storm's mid-levels (especially near minimum  $\theta_e$ ), and
- Storms possessing rotation.

Another microburst nowcasting technique is to monitor for secondary convection (enhancements to the lift process to gain deeper convection) by observing the following on the WSR-88D radar and/or satellite imagery:

- Sea breeze movement and HCR interaction and
- Colliding or intersecting convergent boundaries.

## 4. VERIFICATION TECHNIQUES AND RESULTS

The following sub-sections describe the techniques used in verifying MDPI and WINDEX and the results of the predicted versus observed conditions.

### 4.1 MDPI Verification

MDPI was designed such that values of 1.0 or greater suggest a high likelihood of wet microbursts, assuming development of deep convection with moderate to heavy precipitation.

Because of the large surface temperature lapse on the early morning (1100 UTC) Cape Canaveral rawinsonde and the tropical air mass (Central Florida vs. Northern Alabama), the maximum  $\theta_e$  was calculated using the lower 150 mb (Roeder 1995) and a higher CT value is used for calibration (Wheeler 1995). Both of these changes were modified locally from the work Atkins and Wakimoto had done in the MIST project.

To verify the performance of MDPI as a categorical forecast for microburst potential at KSC and CCAS, data were archived from 1 June to 30 September 1995. Analyses indicated that there were a total of 33 possible microburst events in the KSC/CCAS area during that 4 month period. To determine the skill of the MDPI, a contingency table of MDPI versus observed conditions was developed (Table 1). The analysis consisted of first checking to see if the RWO forecaster had forecast and observed a thunderstorm at the SLF. If so, then a MDPI was computed. Archived wind sensor data were then analyzed for all days to check for peak wind speeds of 30 knots or greater. In addition to helping in the



On 8 September 1995, high pressure was present over Florida, with light southwest surface winds. With the southwest wind flow, HCRs began developing around 1500 UTC to the southwest of Cape Canaveral and extending south toward Melbourne. An east coast sea breeze began developing around 1630 UTC with thunder later heard at the SLF around 1700 UTC. The first thunderstorm was reported at 1921 UTC. At 1955 UTC a wet microburst (47 kt) occurred just north of Highway 528. Figure 16 shows a high VIL (48) over Merritt Island just north of Highway 528. Figure 17 is a classic vertical cross section of a cell with severe characteristics (strong inflow, bounded weak echo region, cloud overhanging, and a precipitation core up to the dry air at 17000 ft). The wet microburst cell developed from a series of thunderstorm cells that were developing along the convergence of the HCRs and the SBF.

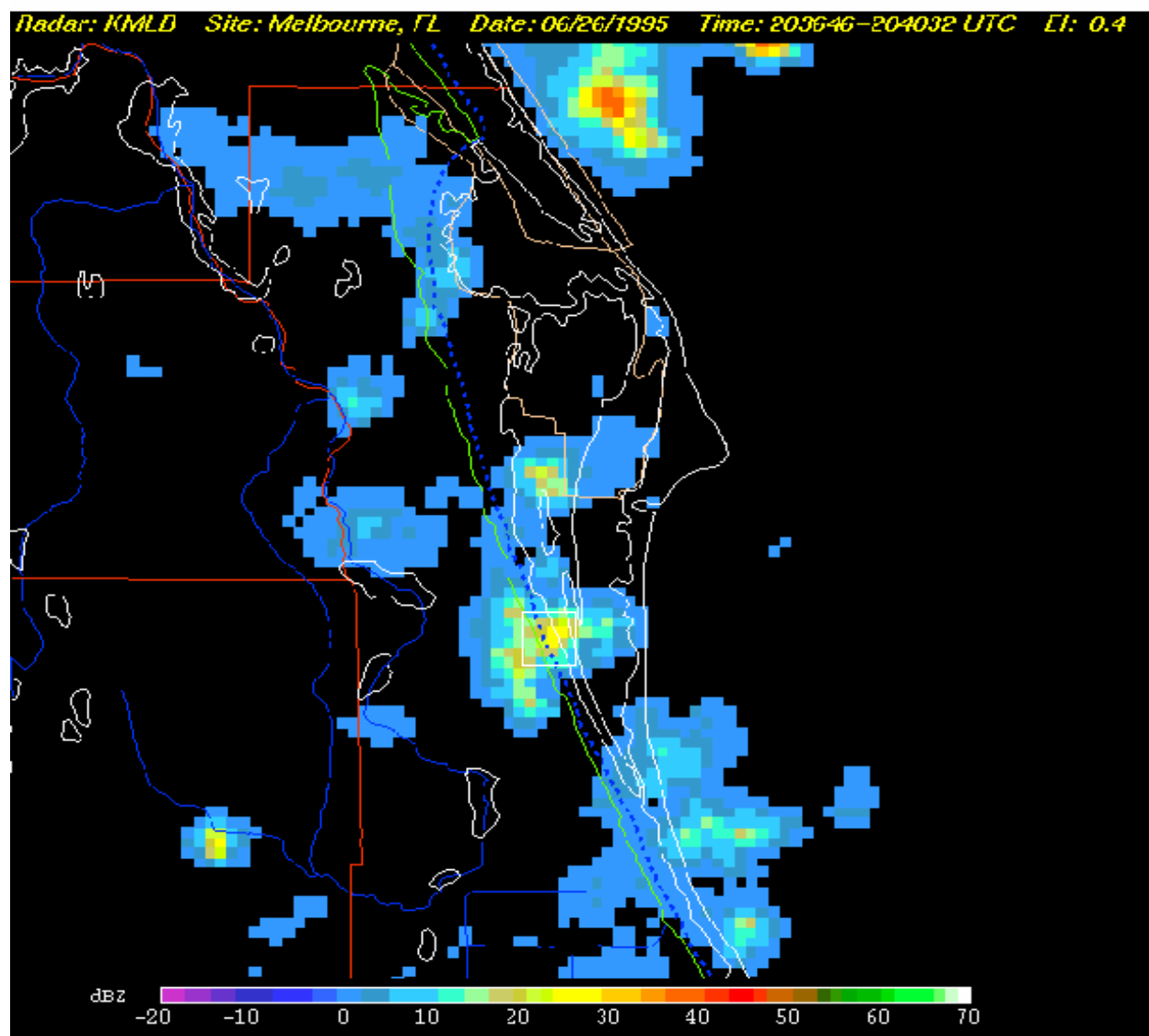


Figure 12. WSR-88D VIL at 2036 UTC on 26 June 1995.

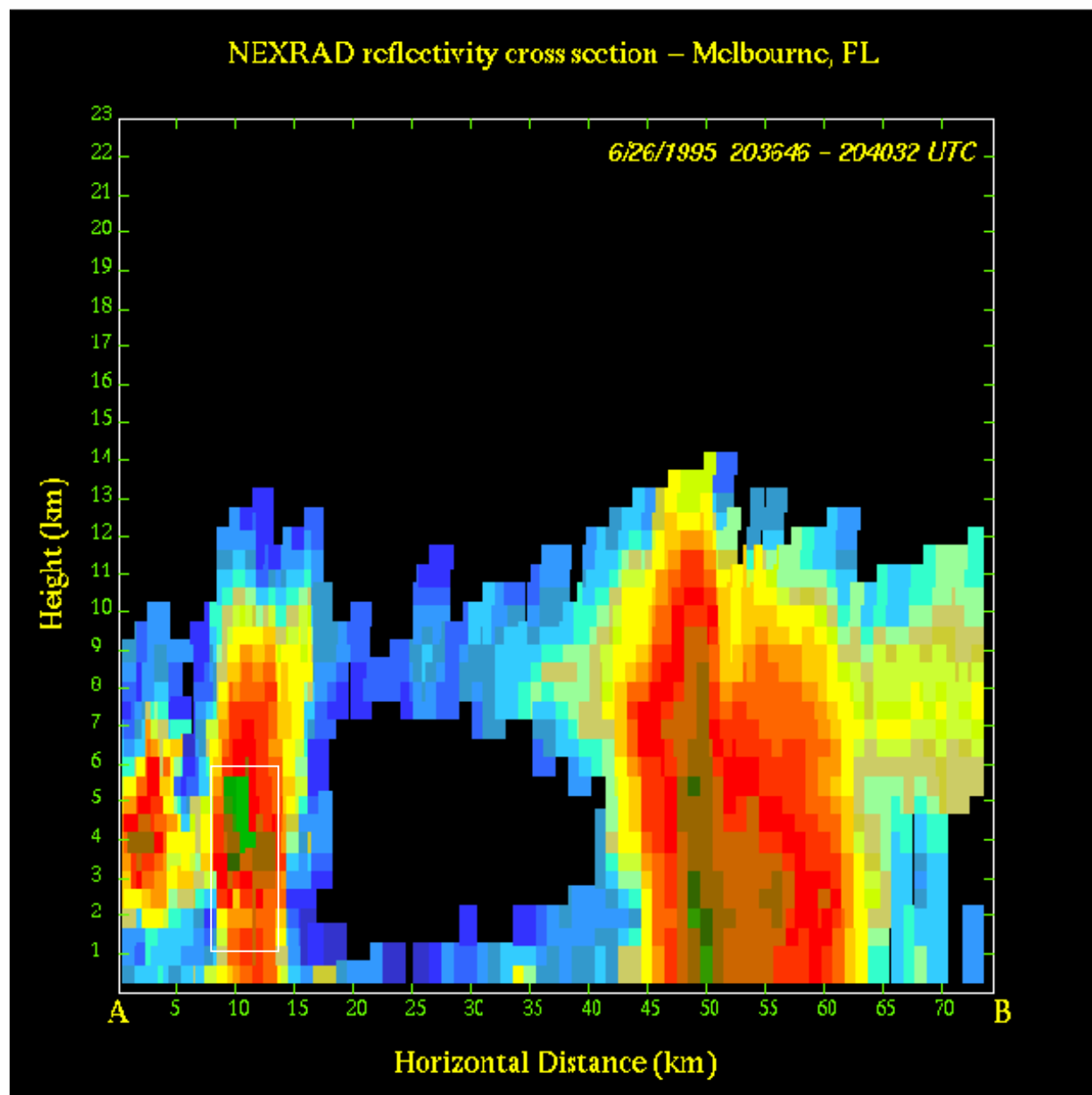


Figure 13. WSR-88D reflectivity cross-section at 2036 UTC on 26 June 1995 (precipitation core is highlighted).

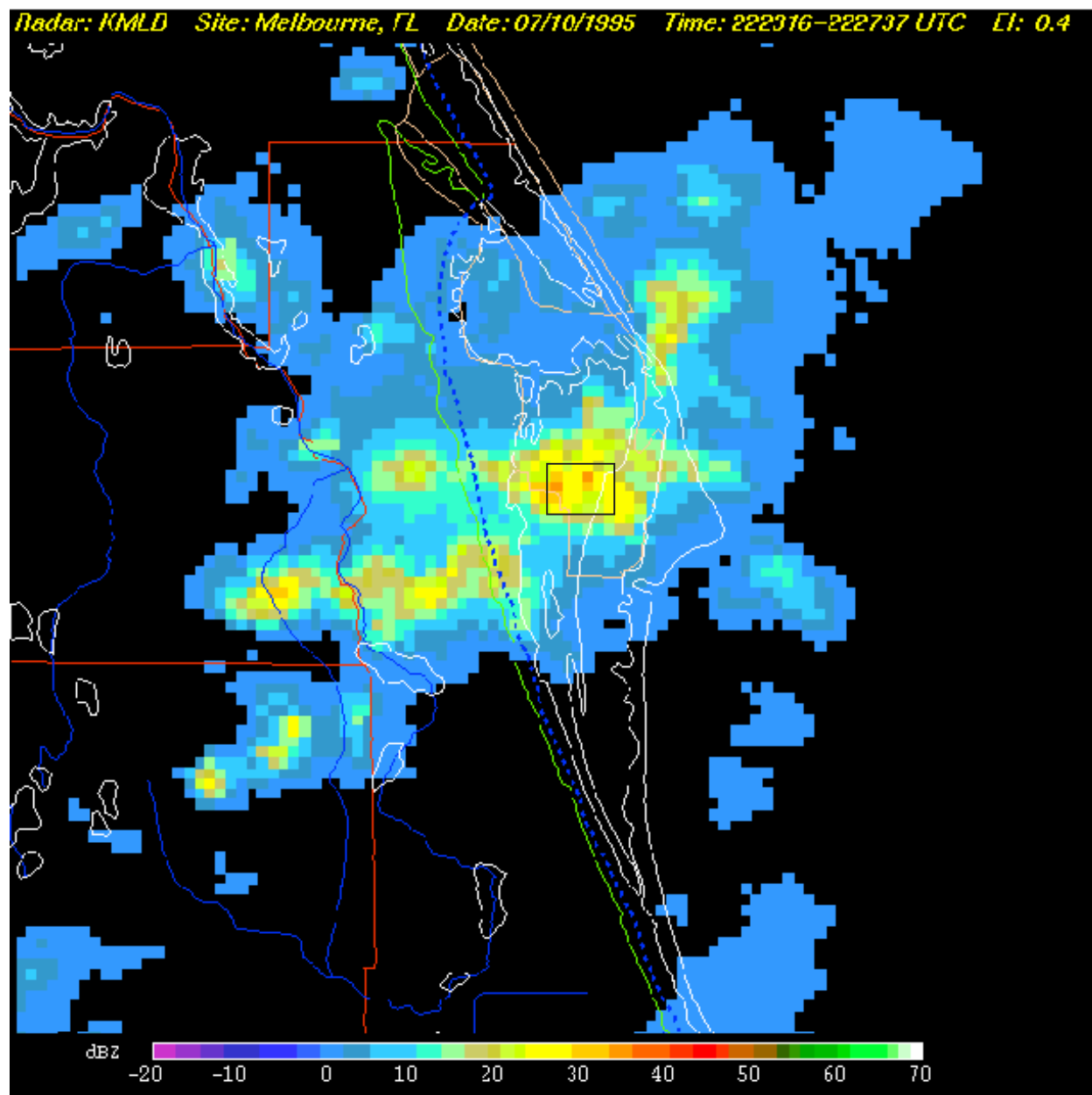


Figure 14. WSR-88D VIL at 2223 UTC on 10 July 1995 (46 dBZ VIL core center is highlighted).

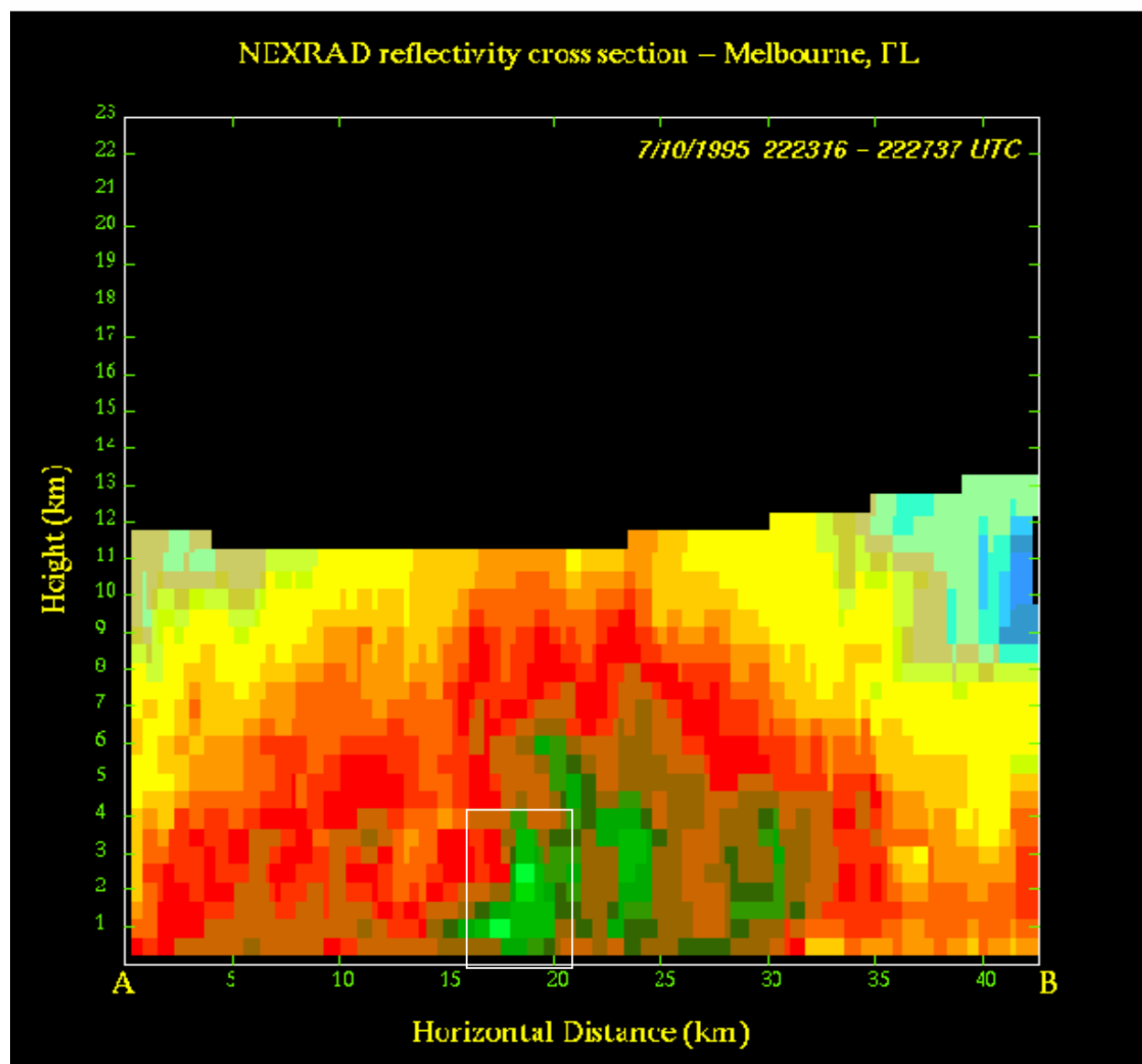


Figure 15. WSR-88D reflectivity cross-section at 2223 UTC 10 July 1995 (precipitation core highlighted).

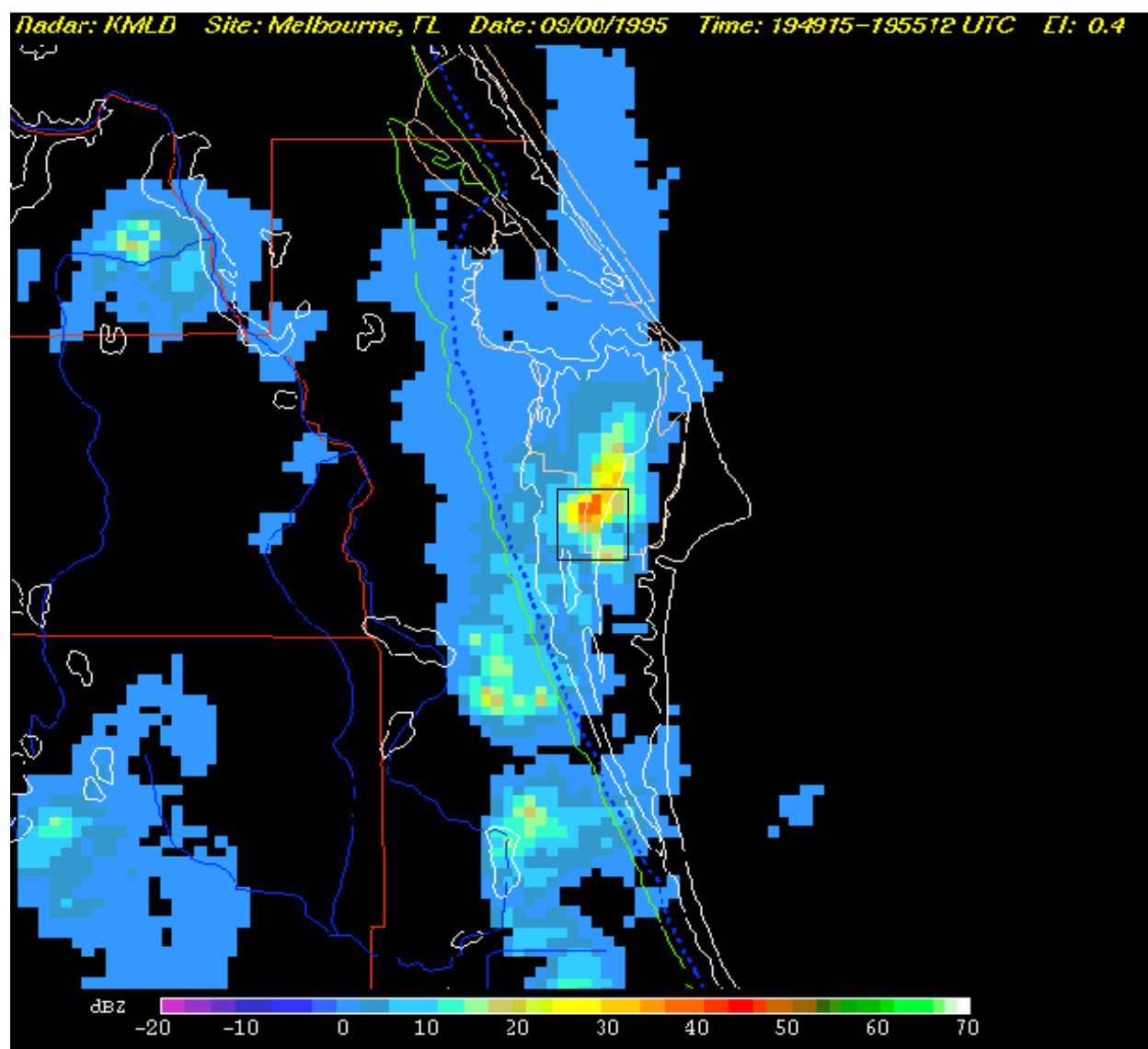


Figure 16. WSR-88D VIL at 1949 UTC on 8 September 1995 (46 dBZ VIL core center is highlighted).

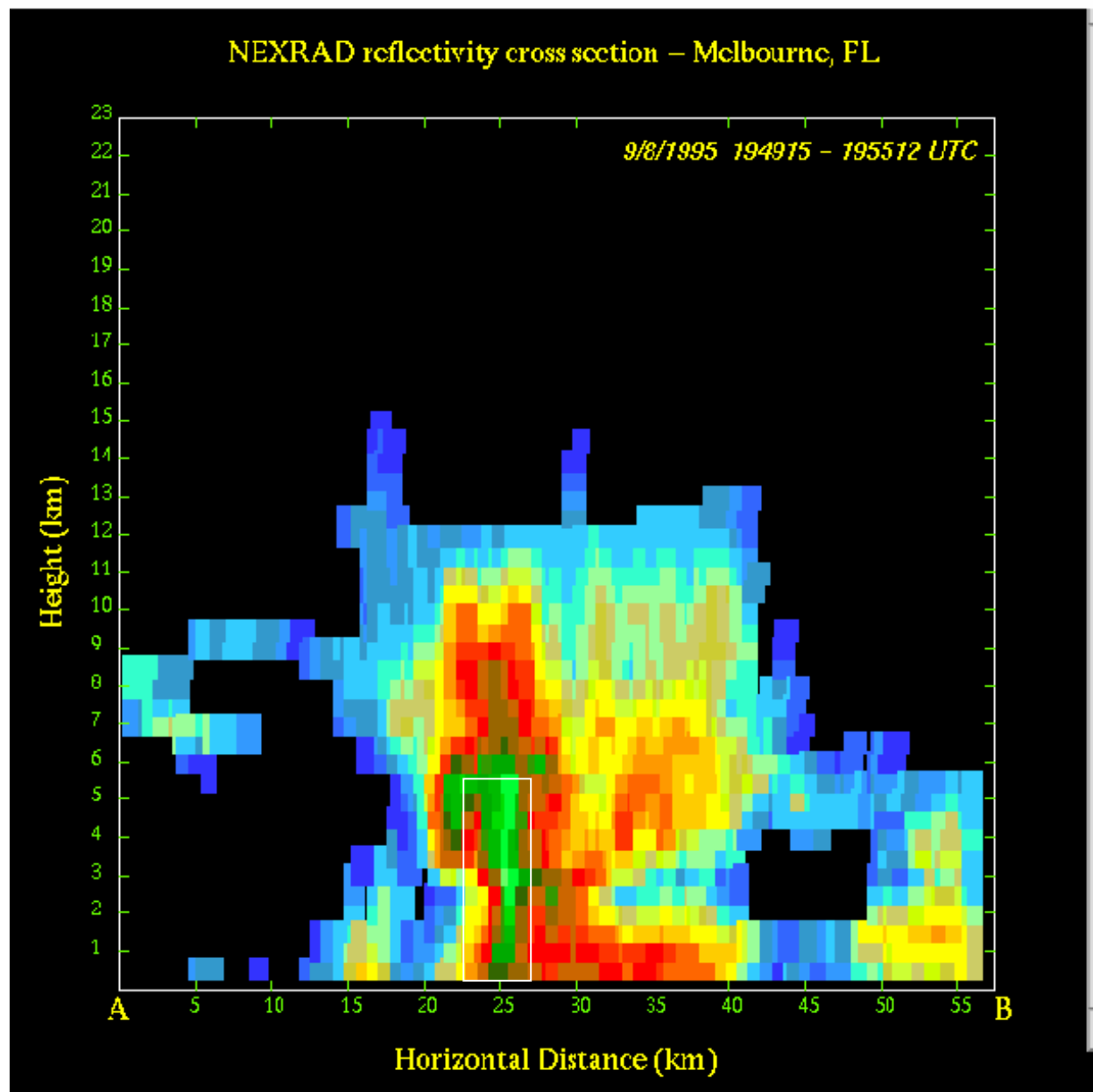


Figure 17. WSR-88D reflectivity cross-section at 1949 UTC on 8 September 1995 (precipitation core is highlighted).

### 4.3 WINDEX Verification

The WINDEX analysis and evaluation was performed using the rawinsonde archived data from 1 June to 30 September 1995. The SKEWTN program was executed on each of the two early morning Cape Canaveral rawinsonde (normally 1000 and 1500 UTC, if available) to calculate the WINDEX gust potential values.

The WINDEX re-analysis based on the hourly SLF surface observation data could not be done efficiently so only a few cases were re-evaluated based on the hourly SLF surface temperature and dew point temperature input. Table 2 shows the rawinsonde-based WINDEX values along with the re-computed surface-based values. Based on this hourly analysis, the trend in the WINDEX forecasted wind gust does show potential value. Three of the four cases randomly selected did show good potential in forecasting the observed wet microburst gust maximum (Bold numbers show forecasted versus observed wind values).

Table 2. Computed WINDEX Microburst Gust vs. Observed Gust							
Date	Time (UTC)	Rawi WINDEX	Sfc WINDEX	Time	Rawi WINDEX	Sfc WINDEX	Observed UTC
12 Jun 95	1000	29	30	2215	48	<b>50</b>	
	1500	58	59	2300	48	<b>45</b>	<b>51 kt at 2320</b>
21 Jul 95	1100	45	44	1900	60	65	
	1500	56	59	2000	56	59	
	1700	60	63	2100	56	30	39 kt at 2100
24 Aug 95	1000	41	42	1800	41	47	
	1600	41	43	1900	41	<b>43</b>	RW began
	1700	41	49	2000	41	41	<b>43 kt at 2030</b>
8 Sep 95	1000	25	24	1700	45	48	
	1500	45	44	1800	45	<b>47</b>	
	1600	45	43	1900	45	<b>44</b>	<b>47 kt at 1955</b>

## 5. RECOMMENDATIONS

The MDPI forecasting technique and WINDEX gust potential value are new tools to be used to alert the KSC/CCAS community of the potential of wet microburst winds and increase the forecaster's vigilance for nowcasting signatures. The MDPI values do show skill in forecasting the potential for microbursts in the Cape Canaveral area. The WINDEX routines were not available until late in the analysis phase of this investigation. Based on just the 1000 and 1500 UTC rawinsondes from the Cape Canaveral WINDEX showed very limited skill in predicting the maximum wind gust from microbursts. However, WINDEX did show skill in alerting the forecaster to the gust potential trend when updated hourly with the current surface observations. WINDEX should be studied in near real time taking into account the surface-based parameters that could further clarify the potential range of microburst wind gust.

## 6. SUMMARY

This report details the research, development, utility, verification and transition on wet microburst forecasting and detection the AMU did in support of ground and launch operations at KSC and CCAS.

The unforecasted wind event on 16 August 1994 of  $33.5 \text{ ms}^{-1}$  (65 knots) at the SLF raised the issue of wet microburst detection and forecasting. The AMU researched and analyzed the downburst wind event and determined it was a wet microburst event. A program was developed for operational use on the MIDDS weather system to analyze, compute and display  $\theta_e$  profiles, the MDPI, and WINDEX maximum wind gust value. Key microburst nowcasting signatures using the WSR-88D data were highlighted. Verification of the data sets indicated that the MDPI has good potential in alerting the duty forecaster to the potential of wet microburst and the WINDEX values computed from the hourly surface data do have potential in showing a trend for the maximum gust potential. WINDEX should help in filling in the temporal hole between the MDPI on the last Cape Canaveral rawinsonde and the nowcasting radar data tools.

## 7. REFERENCES

- Atkins, N. T., and R. M. Wakimoto, 1991: Wet microburst activity over the Southeastern United States: Implications for Forecasting. *Wea. Forecasting*, **6**, 470-482.
- Atkins, N. T., and R. M. Wakimoto, 1995: Observations of the Sea-Breeze Front during CaPE. Part II: Dual-Doppler and Aircraft Analysis. *Monthly Wea Review* **123**, 944-969.
- Eilts, M. and S. Oakland, 1989: Convergence Aloft as a Precursor to Microburst. *24th Conference on Radar Meteorology*, P9.8, 190-193.
- Fujita, T. T., 1985: The downburst: Microburst and Macrobust. SMRP Res. Paper No. 210 (NITIS PB 85-148880). 122 pp.
- Isaminger, M. A. 1988: A Preliminary Study of Precursors to Huntsville Microburst. *Lincoln Laboratory Project Report ATC-153*, 21 pp.
- McCann, D., 1994: WINDEX - A New Index For Forecasting Microburst Potential. *Wea. Forecasting*; **9**, 532-541.
- Roeder, W., 6 September 1994a: AMU Microburst Analysis. *Memorandum for 45 WS/DO*.
- Roeder, W., 24 November 1994b: Microburst Evidence. *Memorandum for 45 WS/DO*.

Roeder, W., 27 January 1995: McIDAS Microburst Utility. *Memorandum for AMU*.

Wakimoto, R. M., 1985: Forecasting dry microburst activity over the High Plains. *Mon. Wea. Rev.*, **113**, 1131-1143.

Wakimoto, R. M., and V. N. Bringi, 1988: Operational detection of microbursts associated with intense convection: The 20 July case during the MIST project. *Mon. Wea. Rev.*, **116**, 1521-1539.

Wheeler, M., 19 November 1994: Analysis and Review of Downrush Wind Events on 16 August 1994. *AMU Memorandum, KSC FL*, 22 pp.

Wheeler, M., 20 July 1995: MDPI Guide. *AMU Memorandum for 45 WS*.

Wolfson, M., 1990: Understanding and Predicting Microburst. *16th Conference on Severe Local Storms, 1990*.